

## ORIGINAL RESEARCH

# A novel comprehensive energy management model for multi-microgrids considering ancillary services

Mehdi Veisi<sup>1</sup>  | Farid Adabi<sup>1</sup>  | Abdollah Kavousi-Fard<sup>2</sup>  | Mazaher Karimi<sup>3</sup> 

<sup>1</sup>Department of Electrical Engineering, Sanandaj Branch, Islamic Azad University, Sanandaj, Iran

<sup>2</sup>Department of Electrical and Electronics Engineering, Shiraz University of Technology, Shiraz, Iran

<sup>3</sup>School of Technology and Innovations, University of Vaasa, Wolffintie 34, Vaasa, Finland

## Correspondence

Farid Adabi, Department of Electrical Engineering, Sanandaj Branch, Islamic Azad University, Sanandaj, Iran.

Email: [farid.adabi@iaau.ac.ir](mailto:farid.adabi@iaau.ac.ir)

## Funding information

Business Finland with Grant, Grant/Award Number: 27081089141/REDISSET/WP/2704800

## Abstract

This article proposes a novel comprehensive multi-layer power management system (PMS) along with its smart distribution network (SDN) constraints as bi-level optimization to address the participation of multi-microgrids (MMGs) in day-ahead energy and ancillary services markets. In the first layer of the proposed model, optimal programming of MMG-connected SDN is considered, in which Microgrids (MGs) participation in the markets is performed to bidirectionally coordinate sources and active loads along with the operator of MGs. In the second layer, the bidirectional coordination of operators of MGs and SDN, that is PMS, is executed in which energy loss, voltage security, and expected energy not-supplied (EENS) are minimized as weighted sum functions. The problem of the difference between costs and revenues of MGs in markets is minimized subject to constraints of linearized AC-power flow, reliability, security, and flexibility of the MGs. To obtain a single-level model, the Karush–Kuhn–Tucker method is applied, and a hybrid stochastic-robust programming is implemented to model uncertainties associated with the load, renewable power, energy price, mobile storage energy demand, and network equipment accessibility. The contributions of this paper include the simultaneous modelling of several economic indicators, multi-layer energy management modelling, and stochastic mixed modelling of uncertainties. The efficiency of this method is validated by simultaneously evaluating the optimum condition of technical and economic indices of several SDNs and MGs. Flexibility of 0.022 MW is obtained for the proposed scheme, which is close to zero (100% flexibility). The voltage security index is increased to 22 by the mentioned scheme, which is close to its normal value, that is, 24. The voltage deviation is below 0.07 p.u. Energy losses are reduced by about 30% compared with that in power flow studies, and the EENS reaches roughly 3 MWh, that is, close to zero (100% reliability).

## 1 | INTRODUCTION

Nowadays, emerging eco-friendly technologies like electric vehicles (EVs) along with renewable resources in power systems lead to clean energy supply conditions and avoid immediate fossil fuel depletion. Non-renewable resources like fuel cells are also utilized due to their low level of emission for supplying power in consumer points. Besides, researchers and operators take the usage of energy storage systems and demand response programs (DRPs) in power systems into account [1]. To attain pleasant environmental status and amend technological and financial aspects of energy, a proper energy management system

is required to handle the aforementioned components. To do such, micro-grids (MGs) including resources, loads, local controllers, and storage devices are introduced to coordinate these various components [2], and then, different MGs are gathered in a distribution network. In addition, a central controller, that is, MG operator (MGO), is considered to bidirectionally coordinate resources, storage devices as well as loads via a smart and communication structure [3]. As a result, a capable MG is provided that can tackle financial and technological issues like security, reliability, and operation via employing an energy or power management system (EMS or PMS) [4]. Moreover, multiple MGs, that is, multi-MGs (MMGs), are presumed here for

This is an open access article under the terms of the [Creative Commons Attribution-NonCommercial License](https://creativecommons.org/licenses/by-nc/4.0/), which permits use, distribution and reproduction in any medium, provided the original work is properly cited and is not used for commercial purposes.

© 2022 The Authors. *IET Generation, Transmission & Distribution* published by John Wiley & Sons Ltd on behalf of The Institution of Engineering and Technology.

bidirectional distribution system operator (DSO) coordination; consequently, an appropriate condition for DSO will be attained [5].

Considerable literature has dealt with managing the distribution grid or MG operation. The voltage security of the distribution grid along with considering EVs was evaluated as an optimization problem in [6], in which maximizing the voltage security margin and minimizing the operational costs were the major objective functions. Besides, bidirectional chargers were considered for EVs that can regulate the real and reactive power of smart grids at the same time. Hybrid electric springs (ESs) and EVs parking lot operation were introduced in [7] to address the intermittent nature of RESs in addition to alternative uncertainties to securely construct a novel MG. This was addressed by a hybrid stochastic/robust programming problem. Also, uncertainties of load, price of energy, RESs, and MG component accessibility were modelled using stochastic programming, and uncertain EVs parking lot parameters were propounded by robust optimization to improve MG indicators. For investigating the RES uncertainties in managing the stored or real/reactive power of an energy storage system with an MG, a robust max-min particle swarm optimization (PSO)-based model was offered in [8], in which maximizing social welfare (SW) was suggested for robust programming of the stored or real/reactive power in MGs. A medium priority was achieved by this robust platform compared to deterministic and stochastic models. Day-ahead and real-time energy market-based bilevel operation of grid-connected MG in addition to various RESs and EVs was proposed in [9] with multi-layer EMS. As MGs were divided into individual or community categories (MGC), both EMS layers were utilized in both categories by their hourly operation in the day-ahead market. In this regard, minimizing the operating costs of MG was conducted in the first step by considering constraints of storage, grid model, EVs parking lot, and distributed generations. Also, the minimization of expected operation and risk aggregated costs of the MGC was conducted in the second layer subject to the same aforementioned constraints. Besides, the minimization of unbalanced cost among day-ahead and real-time operation was done in this layer by assuming 5-min real-time dispatch-based MGs and their components model constraints.

Ref. [10] introduces an energy management system that can achieve the optimal multi-objective operation of MGs and distributed generations with a thermal block with combined heat and power (CHP) plant, thermal storage, and boiler to supply the demand. The three main objectives of this paper were minimization of the cost and energy loss of MG as well as voltage deviation by considering constraints of distributed generations, thermal block, AC power flow, and operation limits of the system. To ameliorate reliability, operation, economic, and emission indicators at the same time, an EMS was recommended as a four-objective optimization problem in [11] for unbalanced MGs with active loads (ALs) along with active and reactive resources. In this work, expected operating cost, expected emission level, expected energy not-supplied (EENS), and voltage deviation function of the MGs and sources were consecutively addressed in the first to fourth levels. UMGs imbalance case, sources and ALs formulation, reliability as well as optimal power

flow equations were assumed as the constraints. Ref. [12] proposed a stochastic multi-layer EMS for linked MGs in smart distribution grids. To define a proper program for MGs, managing energy was realized for individual MGs. The received data was implemented by the smart grid operator to provide a priority list in which power should be injected by each unit; consequently, global energy management was attained. A united heat/real/reactive power programming-based model was presented in [13] for an MG constrained optimal operation in either grid-connected or islanded mode. To supply reactive power according to a reactive power payment function, diesel generators, fuel cells (FCs), and microturbines (MTs) were added to the MG and the produced heat and real power dependency of CHP along with the produced real and reactive powers dependency of alternative units were considered in the MGs optimal economic dispatch as well. The robust strategy of coordinated operation was suggested in [14] by taking operation modes and practical constraints into account for operating cost minimization by coordinating multiple components in various timescales. Also, a robust optimization strategy was expanded to ensure optimal and credible delivery in presence of uncertainties. The EMS for a luxury ship electrical system was studied by authors of [15] to reduce the permanent magnet synchronous generators (PMSG)-based diesel engine fuel consumption of driven to reduce the emitted pollution of a ship. An MG optimal programming model was proposed in [16] and the distribution market operator was considered a participant. The surveyed studies in this field are summarized and classified in Table 1.

Table 1 provides a brief overview of various models of EMS for MGs and distribution grids. Nevertheless, the following gaps should be fulfilled in EMS of MGs and distribution grid:

- Firstly, united or single-layer EMS approaches have been usually used in the literature in which resources, active loads, as well as the DSO direct coordination have merely been presumed. Besides, considering such coordination in MMGs and distribution grid produces a great deal of information for the DSO, leading to complicated decision-making and system process. Thus, two-layer EMS strategies are the optimal and appropriate choice for handling the power of distribution grids with MMGs, in which MGO, resources and active loads coordination can be performed by an EMS layer, and the DSO and MGOs coordination will be conducted by another layer. This can accelerate the speed of process of operators and decision-making. This has been surveyed in only few studies [9, 12].
- Concerning the aforementioned overview, technical conditions of the distribution network can be enhanced by employing EMS in MGs, leading to the participation of MGs in various energy markets and enhancement of their profit. Nevertheless, the energy market model has mostly been utilized for MGs in previous works. As MGs employ generator-based resources like MTs or inverter-based components like RESs, EVs as well as storage, real and reactive power can be controlled at the same time [17], leading to energy market participation as well as active ancillary services markets participation, that is, participating in reactive ancillary services or reserve regulation.

**TABLE 1** Latest literature classification

Ref.	Market model	PMS strategy	Indices	Uncertainty model
[6]	—	One-layer	Operation and security	Deterministic
[7]	—	One-layer	Operation, security, reliability and flexibility	HSRP
[8]	—	One-layer	Operation	Robust
[9]	Energy	Two-layer	Operation and economic	Stochastic
[10]	—	One-layer	Operation and economic	Stochastic
[11]	—	Two-layer	Operation, reliability, emissions, and economic	Stochastic
[12]	—	One-layer	Operation	Stochastic
[13]	—	One-layer	Operation	Stochastic
[14]	—	One-layer	Operation	Robust
[15]	—	One-layer	Operation	Stochastic
[16]	Energy	One-layer	Operation and economic	Stochastic
<b>Proposed strategy</b>	<b>Energy, reactive, and reserve</b>	<b>Two-layer</b>	<b>Operation, economic, security, reliability, and flexibility</b>	<b>HSRP</b>

- The majority of research has considered the optimal state of one or two indicators like financial or operation indicators [6, 8–10, 12–16], while one grid has diverse constraints such as security, operation, reliability, flexibility, and other indexes. Reaching an appropriate condition for a special index does not necessarily ensure enhancement in other indices. Therefore, it would be desirable to simultaneously evaluate various index models of an EMS.
- Most of the research has employed stochastic programming to model uncertainties [9–13, 15, 16]; however, a significant number of scenarios are required in this method for achieving a reliable solution, which demands high computational time. It is worth mentioning that low computational time is of particular importance in operating problems where the operating step is small (even 15 min) [7]. So, robust programming methods have been introduced in some works [8, 14] to model uncertainties. However, several scenarios attained about the accessibility uncertainty of network components (renewable power) are required for the accurate calculation of some indicators, such as EENS (flexibility). Therefore, stochastic modelling of these uncertainties is needed in some circumstances. Therefore, it is expected to adopt a hybrid robust-stochastic programming method for accurate modelling of uncertainties and indicators along with achieving low computational time, which has been discussed less in previous studies.

This paper offers the SDN in the presence of MMGs participation in the energy and ancillary services markets by a two-layer PMS, which is illustrated in Figure 1. The upper level of the suggested strategy considers the bidirectional coordination among the MGO, loads, storage, and resources, and the second layer deals with bidirectional coordination among the DSO and MGOs. As the first layer investigates the optimum programming model of the SDN-connected MMGs according to PMS of the lower level, that is, the coordination among the DSO and MGOs, it is therefore a two-level problem. The MMGs participation formulation in the reserve, reactive power, and day-ahead energy markets in the second layer is

formed with regard to the PMS of the upper level, which is based on the MGO, resources, and active loads coordination. Minimizing the overall energy loss and maximizing network security and reliability are the major goals of the objective function in the first layer, which are modelled using the Pareto optimization based on the weighted sum functions approach. In addition, voltage security, the AC power flow equations, and reliability are its constraints. Minimizing the difference between the MGs expected cost and revenue in the aforementioned markets is the aim of the second layer, which is subject to flexibility, security, and reliability of MGs, reserve model of the MG, DRP, renewable and non-renewable resources equations, AC power flow equations, and active loads like storages and EVs parking lot. The Karush–Kuhn–Tucker (KKT) method is implemented to find a unique and single-level model. To convert this multi-level problem into a single-level one, the convergence of the problem in the second layer is essential for utilizing the KKT and other methods. The AC power flow equations are constraints of the aforementioned problem, so the problem is non-convergent [15, 16]. A linearized method can be employed in the suggested strategy to address the issue that AC power flow equations are replaced by linearized AC ones. To model the uncertainties of market price, load consumption, power generation of renewables, network component accessibility, and EVs energy demand, hybrid stochastic-robust programming is integrated. In this programming, the uncertainties of renewable power and network component accessibility are modelled by stochastic programming to accurately calculate the reliability and flexibility indicators. Firstly, multiple scenarios are generated by the roulette wheel mechanism (RWM) for the aforementioned uncertainties. Next, a specific number of the produced scenarios that have a small distance from each other are selected by the simultaneous backward strategy to be implemented in the problem. In addition, other uncertainty parameters of this paper are modelled according to boundary uncertainty-based robust optimization (BURO). In this strategy, only one scenario, that is, the worst-case scenario, is required; hence, the computational time is short.

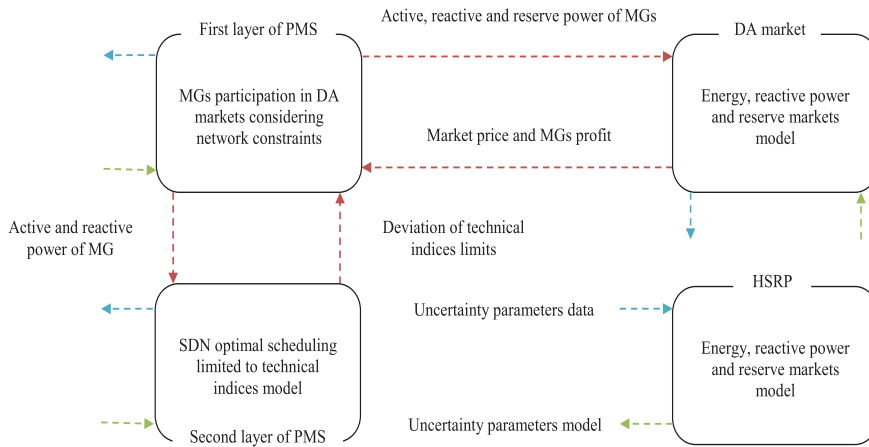


**FIGURE 1** The SDN operation diagram in two-layer PMS-based MGs

The main contributions of this paper can be abstracted as:

- Presenting a bi-level optimization model for the operation of SDN-connected MGs considering technical (operation, reliability, and security) objectives for DSO and flexible MGs operators, while these MGs can obtain profit from DA reserve, reactive power, and energy markets.
- Uncertainty modelling in accordance with hybrid stochastic-robust programming for accurate calculation of flexibility and reliability indicators with achieving low computational time.

The remained of this paper is organized as follows. Section 2 describes the bilevel formulation of the suggested strategy based on the hybrid stochastic-robust model. Section 3 presents its single-level model. The obtained results are evaluated in Section 4. Eventually, Section 5 concludes the paper.

in this subsection. The upper layer coordinates the MGO with loads, storage, and resources of MG, while the lower-level coordinates MGOs with the DSO. Two-level optimization is employed based on this scheme; the first layer minimizes the voltage security index (VSI), EENS, and loss of energy of MGs in SDN by forming a three-objective function with weighted sum functions based on the Pareto optimization that is subject to linearized AC power flow as well as voltage security and reliability constraints. In fact, the first layer handles the lower layer of power management. Moreover, the second layer problem considers the MGs participation formulation in the aforementioned markets proportional to the upper-level PMS. Minimization of the difference among costs and revenue in the aforementioned markets is the aim of objective function that is subject to constraints of flexibility, reserve, voltage security, reliability, and linearized AC power flow equations. Therefore, the proposed strategy mathematical model can be described as:

$$\begin{aligned}
 \min F_1 = & \vartheta_{EEL} \sum_{\omega \in O_S} \pi_{\omega} \left\{ \overbrace{\sum_{b \in O_B} \sum_{t \in O_{OH}} P_{DSb,t,\omega} + \sum_{t \in O_{OH}} \sum_{i \in O_{MG}} P_{MGi,t,\omega}}^{\text{GenerationEnergy}} - \overbrace{\sum_{b \in O_B} \sum_{t \in O_{OH}} L_{Pb,t,\omega}}^{\text{ConsumptionEnergy}} \right\} \\
 & + \vartheta_{EENS} \sum_{\omega \in O_S} \pi_{\omega} \sum_{b \in O_B} \sum_{t \in O_{OH}} L_{NSb,t,\omega} - \vartheta_{VSI} \sum_{\omega \in O_S} \pi_{\omega} \sum_{t \in O_{OH}} WSI_{t,\omega}
 \end{aligned} \quad (1)$$

## 2 | SUGGESTED PROBLEM MODEL

### 2.1 | The bilevel power management of the SDN-connected MGs operation

Participation of MGs presented in SDN in the reserve, reactive power, and DA energy markets by the bilevel PMS is described

Subject to:

$$\begin{aligned}
 & L_{NSb,t,\omega} + P_{DSb,t,\omega} + \sum_{i \in O_{MG}} A_{MGb,i} P_{MGi,t,\omega} \\
 & + \sum_{j \in O_B} A_{Lb,j} P_{Lb,j,t,\omega} = L_{Pb,t,\omega} \quad \forall b, t, \omega
 \end{aligned} \quad (2)$$

$$\begin{aligned} & Q_{DSb,t,\omega} + \sum_{i \in O_{MG}} A_{MGb,i} Q_{MGi,t,\omega} + \sum_{j \in O_B} A_{Lb,j} Q_{Lb,j,t,\omega} \\ & = L_{Qb,t,\omega} \quad \forall b, t, \omega \end{aligned} \quad (3)$$

$$\begin{aligned} P_{Lb,j,t,\omega} = & \left\{ G_{Lb,j} \sum_{p \in O_p} ((s_p - V_{\min}) \Delta V_{b,t,\omega,p} - V_{\min} \Delta V_{j,t,\omega,p}) \right. \\ & \left. - (V_{\min})^2 B_{Lb,j} (\varphi_{b,t,\omega} - \varphi_{j,t,\omega}) \right\} \beta_{Lb,j,\omega} \\ & \quad \forall b, j, t, \omega \end{aligned} \quad (4)$$

$$\begin{aligned} Q_{Lb,j,t,\omega} = & \left\{ -B_{Lb,j} \sum_{p \in O_p} ((s_p - V_{\min}) \Delta V_{b,t,\omega,p} - V_{\min} \Delta V_{j,t,\omega,p}) \right. \\ & \left. - (V_{\min})^2 G_{Lb,j} (\varphi_{b,t,\omega} - \varphi_{j,t,\omega}) \right\} \beta_{Lb,j,\omega} \\ & \quad \forall b, j, t, \omega \end{aligned} \quad (5)$$

$$\varphi_{b,t,\omega} = 0 \quad \forall b = \text{Slack bus of SDN}, t, \omega \quad (6)$$

$$\begin{aligned} & P_{DSb,t,\omega} \cos(m \cdot \Delta\theta) + Q_{DSb,t,\omega} \sin(m \cdot \Delta\theta) \\ & \leq \bar{S}_{DSb} \beta_{DSb,\omega} \quad \forall b = \text{Slack bus of SDN}, t, \omega, m \end{aligned} \quad (7)$$

$$P_{Lb,j,t,\omega} \cos(m \cdot \Delta\theta) + Q_{Lb,j,t,\omega} \sin(m \cdot \Delta\theta) \leq \bar{S}_{Lb,j} \quad \forall b, j, t, \omega, m \quad (8)$$

$$0 \leq \Delta V_{b,t,\omega,p} \leq \frac{V_{\max} - V_{\min}}{n_p} \quad \forall b, t, \omega, p \quad (9)$$

$$0 \leq L_{NSb,t,\omega} \leq L_{Pb,t,\omega} \quad \forall b, t, \omega \quad (10)$$

$$\begin{aligned} WSI_{t,\omega} = & (V_{\min})^4 + \sum_{p \in O_p} s'_p \Delta V_{pb-1,t,\omega,p} - 4(V_{\min})^2 \\ & \times \{ R_{pb-1,pb} P_{Lpb-1,pb,t,\omega} + X_{pb-1,pb} Q_{Lpb-1,pb,t,\omega} \} \quad \forall t, \omega \end{aligned} \quad (11)$$

$$WSI_{t,\omega} \geq WSI^{\min} \quad \forall t, \omega \quad (12)$$

$$\begin{aligned} P_{MGi,t,\omega}, Q_{MGi,t,\omega} \in \arg \left\{ \min F_2 = \sum_{\omega \in O_S} \pi_{\omega} \sum_{i \in O_{OH}} \right. \\ \left. \times \left\{ \sum_{i \in O_{MG}} \sum_{b \in O_B^{MG}} \beta_{i,b} P_{NRi,b,t,\omega} \right. \right. \\ \left. \left. - \sum_{i \in O_{MG}} \gamma_{t,\omega} (P_{MGi,t,\omega} + K_Q Q_{MGi,t,\omega} + K_R R_{MGi,t,\omega}) \right\} \right\} \end{aligned} \quad (13)$$

Subject to:

Constraints (4) – (12) with adding index to all parameters and variables, and substituting  $DS$  to  $MG \quad \forall i$  (14)

$$\begin{aligned} & L_{NSi,b,t,\omega} + P_{MGi,b,t,\omega} + P_{NRi,b,t,\omega} + P_{Ri,b,t,\omega} + P_{DRi,b,t,\omega} \\ & + (P_{DISi,b,t,\omega} - P_{CHi,b,t,\omega}) + \sum_{j \in O_B^{MG}} A_{Lb,j} P_{Li,b,j,t,\omega} \\ & = L_{Pb,b,t,\omega} \quad \forall i, b, t, \omega, P_{MGi,t,\omega} = P_{MGi,b=\text{slackbusof}MG,t,\omega} \end{aligned} \quad (15)$$

$$\begin{aligned} & Q_{MGi,b,t,\omega} + Q_{NRi,b,t,\omega} + Q_{Ri,b,t,\omega} + Q_{Ei,b,t,\omega} \\ & + \sum_{j \in O_B^{MG}} A_{Lb,j} Q_{Li,b,j,t,\omega} = L_{Qi,b,t,\omega} \quad \forall i, b, t, \omega, Q_{MGi,t,\omega} \\ & = Q_{MGi,b=\text{slackbusof}MG,t,\omega} \end{aligned} \quad (16)$$

$$-\xi_{i,b} L_{Pb,b,t,\omega} \leq P_{DRi,b,t,\omega} \leq \xi_{i,b} L_{Pb,b,t,\omega} \quad \forall i, b, t, \omega \quad (17)$$

$$\sum_{t \in O_{OH}} P_{DRi,b,t,\omega} = 0 \quad \forall i, b, \omega \quad (18)$$

$$\begin{aligned} \underline{E}_{i,b} \leq IE_{i,b} + \sum_{t'=1}^t \left( \eta_{CH} P_{CHi,b,t',\omega} - \frac{1}{\eta_{DIS}} P_{DISi,b,t',\omega} \right) \\ \leq \bar{E}_{i,b} \quad \forall i, b, t, \omega \end{aligned} \quad (19)$$

$$0 \leq P_{CHi,b,t,\omega} \leq \alpha_{CRi,b} \quad \forall i, b, t, \omega \quad (20)$$

$$0 \leq P_{DISi,b,t,\omega} \leq \alpha_{DRi,b} \quad \forall i, b, t, \omega \quad (21)$$

$$\begin{aligned} & (P_{DISi,b,t,\omega} - P_{CHi,b,t,\omega}) \cos(m \cdot \Delta\theta) + Q_{Ei,b,t,\omega} \sin(m \cdot \Delta\theta) \\ & \leq \bar{S}_{Ei,b} \quad \forall i, b, t, \omega, m \end{aligned} \quad (22)$$

$$P_{Ri,b,t,\omega} \cos(m \cdot \Delta\theta) + Q_{Ri,b,t,\omega} \sin(m \cdot \Delta\theta) \leq \bar{S}_{Ri,b} \quad \forall i, b, t, \omega, m \quad (23)$$

$$\begin{aligned} & P_{NRi,b,t,\omega} \cos(m \cdot \Delta\theta) + Q_{NRi,b,t,\omega} \sin(m \cdot \Delta\theta) \leq \bar{S}_{NRi,b} \\ & \quad \forall i, b, t, \omega, m \end{aligned} \quad (24)$$

$$\begin{aligned} & (P_{MGi,b,t,\omega} + R_{MGi,b,t,\omega}) \cos(m \cdot \Delta\theta) + Q_{MGi,b,t,\omega} \sin(m \cdot \Delta\theta) \\ & \leq \bar{S}_{MGi,b} \beta_{MGi,b,\omega} \\ & \quad \forall R_{MGi,b,t,\omega} \geq 0, i, b = \text{Slack bus of MG}, t, \omega, m \end{aligned} \quad (25)$$

$$\sum_{\omega \in O_S} \pi_{\omega} \sum_{b \in O_B^{MG}} \sum_{t \in O_{OH}} \overbrace{L_{NSi,b,t,\omega}}^{EENS_i} \leq EENS^{\max} \quad \forall i \quad (26)$$

$$\begin{aligned} -\Delta F &\leq P_{MGi,b,t,\omega} - P_{MGi,b,t,\omega'} \leq \Delta F \quad \forall i, b \\ &= \text{Slack bus of MG, } t, \omega, \omega' \end{aligned} \quad (27)$$

The first layer formulations are presented in (1)–(12). The Pareto optimization-based three-objective function is the main objective function that utilizes the weighted sum functions, which is given in (1) [11]. Minimizing the SDN-related loss of energy is presented in the first part of Equation (1) and equals the difference between energy generation and consumption in the operation time. Minimization of EENS resulting from the occurrence of  $N-1$  events because of an internal fault in network components is considered as the second term. This energy also equals the aggregation of loads not-supplied in the SDN because of internal faults in various components. Finally, minimization of the VSI symmetry is exhibited in the third part [6]. In this paper, the worst security index (WSI), which is in the range of [0, 1] is utilized for voltage security analysis. If this index equals 1, the SDN is in the no-load condition, and if it equals 0, a voltage drop may have occurred. Additionally, this indicator is considered for a weak bus regarding the magnitude of voltage and results of power flow is implemented to discover this bus. However, maximization of the third term of this equation makes the SDN accessible with high voltage security. Therefore, this term will have a negative coefficient [6].

The weighted sum coefficients, that is,  $\omega_{VSI}$ ,  $\omega_{EENS}$ , and  $\vartheta_{EEL}$  should equal one because Equation (1) is a three-objective function [11]. To achieve this, it is anticipated that VSI, EENS, and EEL functions have various values for various coefficients; its 3D coordinate plane diagram illustrates the suggested strategy Pareto front [11]. The fuzzy decision-making method can be employed here for discovering an optimum point, that is, the best optimum solution of the aforementioned functions [18]. In this method, for various weighted coefficients, a linear membership function is firstly provided for VSI, EENS, and EEL functions. When the value of the function is lower (more) than its upper (lower) boundary, the membership value of each of the functions will be one (zero) [18]; if not, the value equals the difference among the function regarding its upper boundary and the difference among the function's upper and lower boundaries [18]. Considering  $\vartheta_{VSI}$ ,  $\vartheta_{EENS}$ , and  $\vartheta_{EEL} = 1$ , the VSI, EENS, and EEL functions boundaries are obtained. Then, for every weighted coefficient, the least membership value, denoted by  $\vartheta$ , among the aforementioned functions is established. Eventually, the best correspondence point of the aforementioned functions equals the highest  $\vartheta$  value for all selected values of weight coefficients [18].

The first layer limitations are represented in (2)–(12), and the linearized AC power flow limitations in the SDN are shown in (2)–(6) [19–21]. Such limitations define the slack bus voltage angle, real and reactive power flow in the line, and balance between real and reactive power

in each bus. Equations (4) and (5) are non-linear non-convergence real models in the form of  $P_{Lb,j} = G_{Lb,j}(V_b)^2 - V_b V_j \{G_{Lb,j} \cos(\varphi_b - \varphi_j) + B_{Lb,j} \sin(\varphi_b - \varphi_j)\}$  and  $Q_{Lb,j} = -B_{Lb,j}(V_b)^2 + V_b V_j \{B_{Lb,j} \cos(\varphi_b - \varphi_j) - G_{Lb,j} \sin(\varphi_b - \varphi_j)\}$  [19]. Nevertheless,  $\cos(\varphi_b - \varphi_j)$  and  $\sin(\varphi_b - \varphi_j)$  terms are estimated to be 1 and  $(\varphi_b - \varphi_j)$ , respectively, because the difference among near- and far-end bus voltage angles of the distribution line is usually smaller than  $6^\circ$  [20]. In addition, the magnitude of voltage is represented by the traditional piecewise linearization method as  $V_{\min} + \sum_{p \in O_P} \Delta V_p$ , where  $\Delta V$  is the deviation of voltage that can be reduced by employing a piecewise higher number. Then,  $V^2$ ,  $V^4$ , and  $V_b V_j$  are defined as  $(V_{\min})^2 + \sum_{p \in O_P} s_p \Delta V_p (V_{\min})^4 + \sum_{p \in O_P} s'_p \Delta V_p$  and  $(V_{\min})^2 + V_{\min} \sum_{p \in O_P} (\Delta V_{b,p} + \Delta V_{j,p})$ . If  $\Delta V^2$  and  $\Delta V(\varphi_b - \varphi_j)$  are ignored because of their small values, the aforementioned non-linear terms are rewritten like (4) and (5) [21]. The SDN operational limitations are presented in (7)–(9), which consecutively illustrate the limits of voltage deviation on the buses of the SDN as well as constraints of the apparent transferrable power through line and substation of the SDN [22]. The limit on real model of the line and substation capacity can be indicated by a circular plane with a centre on origin and a radius of  $S$ ,  $\sqrt{(P)^2 + (Q)^2} \leq S$ . This plane is approximated by a regular polygon, as  $P \cos(m\Delta\theta) + Q \sin(m\Delta\theta) \leq S$  [22]; as long as the number of sides is big, the calculational error can be ignored. Here,  $m$  denotes the set of sides,  $O_M = \{1, 2, \dots, n_m\}$ , while  $n_m$  and  $\Delta\theta$  represent the number of sides and the angle deviation ( $360/n_m$ ), respectively. The constraints of voltage magnitude in the AC power flow real model are defined as  $V_{\min} \leq V_{b,t,\omega} \leq V_{\max}$ . Voltage magnitude limit is replaced by Equation (9) because voltage deviation is considered in the linearized AC power flow. Moreover, the upstream network is assumed to be connected to SDN via a distribution substation located at the slack bus. So, values of  $P_{DS}$  and  $Q_{DS}$  are available only for the slack bus. Finally, the constraint of SDN reliability is presented by (10), applying to the limits of the interrupted load caused by  $N-1$  events at consumption points. The constraints of SDN voltage security are represented by (11) and (12); the WSI of the weakest bus is computed by (11) and (12) provides the boundary of this index [6]. It means that a secure voltage margin ought to be constantly considered for the SDN, as (12). The WSI real model will be written as  $WSI = (V_{pb-1})^4 - 4(V_{pb-1})^2 \{R_{pb-1,pb} P_{Lpb-1,pb} + X_{pb-1,pb} Q_{Lpb-1,pb}\} - 4\{X_{pb-1,pb} P_{Lpb-1,pb} - R_{pb-1,pb} Q_{Lpb-1,pb}\}^2$ , the two last terms in the above relation are very smaller than the first one [6]; so, this equation is replaced by (12). The first part of (12) shows the  $V^4$  linear model by the traditional piecewise linearization method and the third one is omitted due to its negligible value. Moreover,  $\sum_{p \in O_P} s_p \Delta V_p$  and  $\{R_{pb-1,pb} P_{Lpb-1,pb} + X_{pb-1,pb} Q_{Lpb-1,pb}\}$  is excluded from (12) as well since its multiplication has an ignorable value.

MGs participation in the reserve, reactive power, and energy markets, the problem of the first level, is given in (13)–(27) where the difference among the MGs cost (i.e. the operating

cost of non-renewables in the first term of (13)) and the expected revenues in the aforementioned markets (the second part) are minimized by this objective function. According to its second term, revenue for MGs will be produced if reserve, real, and reactive powers are positive; otherwise, i.e. for a negative value, a cost should be paid by MGs. As noted, constraints (4)–(12) also hold for MGs, and these are considered in (14). Limitations of real and reactive power balance in various buses of MGs with loads, storage, and resources can be given as (15) and (16), respectively. Reactive power can be controlled by (16) that resources and storage are assumed in. As non-renewable resources are generator-based, their reactive power can be regulated by generators, while reactive power of RESs and storage devices can be supervised by implementing a suitable structure for power electronic converters that connect them to the grid [17].

The incentive-based DRP formulation is proposed by (17) and (18) [7]. Here, according to the signal of energy price, the energy consumption of consumers may decrease at peak hours (based on high prices of energy), while they may receive energy in off-peak hours (based on low prices of energy). Thus, the power limitations of consumers in a DRP are represented in (17) and (18) guarantee that the overall decreased energy in peak intervals can be provided during the off-peak hours. Then, the storage operational models are shown as (19)–(22), which consecutively represent stored energy limitations of the storage devices, charge and discharge rates, and capacity of storage chargers [20]. This model can be implemented for mobile storage, that is, EVs, though the number of EVs may differ in every scenario or time. Therefore,  $t$  and  $\omega$  subscripts are applied to  $IE$ ,  $\alpha_{CR}$ ,  $\alpha_{DR}$ , and  $\bar{S}_E$ . In this regard,  $\alpha_{CR}/\alpha_{DR}/\bar{S}_E$  will be the sum of charge and discharge rates and EVs charger capacities that are connected to the parking lot at time  $t$ . At time  $t$ ,  $IE$  equals the aggregation of initial energy of EVs newly linked to the parking lot. An  $\omega$  subscript is considered for  $\bar{E}$  because variable number of EVs in each scenario equals the energy consumption aggregation needed for EVs travel. In this operational model of EVs, the inequality part on the right side of (19) is expressed as equality. The operational model limitations of renewable and non-renewable resources are presented by (23) and (24), showing their apparent power capacity limitations. Employing (25), the reserve power can be computed, which is almost positive. The EENS constraints of every MG are shown in (26). Since the MGs financial objectives in the electricity market are perceived as the objective function, the MGs reliability limit is presented as a similar limitation as (26). The MGs flexibility constraint is considered as (27). As there are prediction errors in forecasting the meteorological data, the RESs real power generation will be uncertain, and the MGs real power (observed from the substation or slack bus) may be different in various scenarios, leading to an imbalance in the DA and real-time operation results [9]. This condition is represented as flexibility shortage status from a financial perspective. The cost imposed by MGs will escalate due to the decreased flexibility penalty. Thus, a limit as (27) is utilized for MGs to prevent this issue; the smaller flexibility tolerance value ( $\Delta F$ ), the higher MGs flexibility, that is, minimization of the MGs real power should be considered in

different scenarios. MGs flexibility status is improved here by ALs and non-renewable resources that are famous as flexibility resources.

In this paper, the power variables model of sources, storage and network is used, and it is assumed that they can obtain the calculated power by adjusting and controlling their internal parameters. Therefore, the details of their adjustment parameters in the problem model are not necessary.

## 2.2 | Hybrid stochastic-robust programming of uncertainties

In the aforementioned equations (1)–(27), renewable power ( $P_R$ ), price of energy ( $\gamma$ ), SDN and MGs components accessibility ( $\beta_{DS}$ ,  $\beta_{MG}$ ,  $\beta_L$ ), EVs consumption energy ( $\bar{E}$ ), charge and discharge rates ( $\alpha_{CR}$ ,  $\alpha_{DR}$ ), EVs initial energy and charger capacity ( $IE$ ,  $\bar{S}_E$ ), and load parameters ( $L_P$ ,  $L_Q$ ) are uncertainty parameters. To model these uncertainties, hybrid stochastic-robust programming is implemented. The reliability indicator (EENS) is here an important index that is not associated with the price of energy, while it strongly depends on the accessibility/inaccessibility of the network components uncertainty [23–26]. In addition, as the EVs load and consumption energy uncertainty alters, it does not mainly change because of their low predicted error. So, stochastic programming can model  $\beta_{DS}$ ,  $\beta_{MG}$ , and  $\beta_L$  uncertainties [23]. Further, different scenarios obtained from the renewable power uncertainty are required to investigate the flexibility state of the network, (27). Thus,  $P_R$  is also modelled based on stochastic optimization. In stochastic programming, so many scenarios are produced by the RWM, where  $P_R$  of any scenario is described by its average and standard deviation. Besides, the forced outage rate (FOR) index of network components and MGs are employed to exploit the three last uncertainties [27, 28]. Additionally, the renewable power probability for wind and photovoltaic systems can be consecutively determined by Weibull and Beta probability density functions [4]. The Bernoulli probability density function will give the probability of  $\beta_{DS}$ ,  $\beta_{MG}$ , and  $\beta_L$  [23]. The event occurring probability in any scenario equals the multiplication of the uncertainty probabilities in that scenario. Then, a few of produced scenarios are selected by the SBM and utilized in the suggested problem. It is worth mentioning that scenarios with a minuscule distance from each other will be chosen (for more details, see [2]).

Other parameters will be modelled by robust programming. In this method, only one scenario is considered, that is the worst scenario obtained by uncertainties of load, energy prices, and EVs. Then, robust programming provides an optimum solution in the aforementioned scenario, which is proportional to the robust solution against mentioned uncertainties. The bounded uncertainty-based robust optimization (BURO) method is employed in this paper for its simple formulation process and optimum accuracy to robustly model the uncertainties [21]. In this method, the true value of the uncertainty parameter,  $\mu$ , is located between the lower and upper boundaries,  $[(1 - \sigma) \times \bar{\mu}, (1 + \sigma) \times \bar{\mu}]$ . Here,  $\bar{\mu}$  represents the expected

value of  $u$ , and  $\sigma$  denotes the level of uncertainty that is proportional to the prediction error [21]. If zero is adopted for  $\sigma$ , the deterministic model of  $u$  is considered, but if  $\sigma > 0$ , a robust model will be assumed for  $u$ . Furthermore, the true value of  $u$  in the worst scenario places on its upper or lower boundary by the BURO method. This issue selection depends on the location of  $u$  in the problem so that less solution space should be obtained in the worst scenario in comparison with the deterministic model scenario [21]. Therefore,  $\bar{E}$ ,  $L_P$ , and  $L_Q$  are located at their upper boundary, while  $\gamma$ ,  $\alpha_{CR}$ ,  $\alpha_{DR}$ ,  $IE$ , and  $\bar{S}_E$  are at their lower boundary.

### 3 | SINGLE-LEVEL MODEL OF THE PROBLEM

To discover an optimum solution for (1)–(27) by conventional solvers, it is necessary to reach a single-level model [29]. The KKT will be implemented in the following to fulfil.

The problem model discussed earlier keeps a general problem structure of (28)–(32). The first- and second-layer problems can be expressed by (28) and (29) and (30)–(32), respectively. The variable vector of the first- and second-layer problems can be described as  $x(y)$ . Parameters  $\rho$  and  $\mu$  indicate the Lagrange multipliers.

$$\min F_1 = a^T x + b^T y \quad (28)$$

Subject to:

$$c_1 x + d_1 y (\leq / = / \geq) e_1 \quad (29)$$

$$y \in \arg \{ \min F_2 = f^T y \quad (30)$$

Subject to:

$$g_1 y = b_1 : \rho \quad (31)$$

$$g_2 y \leq b_2 : \mu \quad (32)$$

To achieve the single-objective model of the discussed problem, the constraints discovered by the second layer problem KKT should be applied to the first layer problem [29]. To do this, the Lagrange function ( $L$ ) of the second layer problem is found as (33) by amalgamating the limitations of objective and penalty functions together. Note that  $\mu \cdot \max(0, a - b)$  and  $\rho \cdot (b - a)$  give the penalty function constraints for  $a \leq b$  and  $a = b$ , respectively [29].

$$L = F_2 + \rho \cdot (b_1 - g_1 y) + \mu \cdot \max(0, g_2 y - b_2) \quad (33)$$

Constraints discovered by the KKT are proportional to Lagrange function derivative making that equals zero by differentiating from its variables ( $y$ ,  $\mu$ , and  $\rho$ ) [29]. Consequently, the single-level problem formulation of (28)–(32) is based on

(34)–(39). Equations (34) and (35) in the recently formulated problem (28), (29) describe the first layer problem. When Lagrange function derivative is 0 with respect to the second layer problem-related initial variable ( $y$ ), Equation (36) can be written. By making  $\frac{\partial L}{\partial \rho} = 0$ , (37) can be found, which is similar to (31); and (38) is a non-linear constraint that can be achieved by  $\frac{\partial L}{\partial \mu} = 0$  ( $\mu$  will be the inequality Lagrange multiplier), which is similar to (32) reached by its initial value.  $\mu \cdot (g_2 y - b_2) = 0$  will be obtained by the second condition. To linearize it,  $-M \cdot z \leq \mu \leq M \cdot z$  along with  $-M \cdot (1 - z) \leq (g_2 y - b_2) \leq M \cdot (1 - z)$  will be involved in  $\mu \cdot (g_2 y - b_2) = 0$ ;  $M$  and  $z$  are big constants like  $10^6$  and a binary variable, respectively [29]. The Lagrange multiplier boundary is provided by (39).

$$\min F_1 = a^T x + b^T y \quad (34)$$

Subject to:

$$\text{Constraint (29)} \quad (35)$$

$$\frac{\partial L}{\partial y} = 0 \Rightarrow g_1 \rho + g_2 \mu = f \quad (36)$$

$$\frac{\partial L}{\partial \rho} = 0 \Rightarrow \text{Constraint(31)} \quad (37)$$

$$\frac{\partial L}{\partial \mu} = 0 \Rightarrow \begin{cases} \text{Constraint (32)} & \forall \text{ First condition} \\ \mu \cdot (g_2 y - b_2) = 0 & \forall \text{ Second condition} \end{cases} \quad (38)$$

$$\rho \in (-\infty, +\infty), \mu \in [0, +\infty) \quad (39)$$

## 4 | NUMERICAL RESULTS

### 4.1 | Case studies

In this section, the surveyed case studies are exclusively analysed. To do so, a typical 69-bus radial SDN [30] with 3 microgrids, namely, MG1, MG2, and MG3, is considered to investigate the suggested method [30]. The MGs are connected to buses 15, 42, and 58, respectively. The information about lines and substations of the SDN, and peak load can be found in [30]; MGs data has been provided in [12]. It is assumed that Bus 1 is the slack bus, while slack buses of MG1, MG2, and MG3 are buses 15, 42, and 58, respectively. The acceptable magnitude of voltage is within [0.9, 1.1] (per-unit) [31–34]. Wind and PV energies are involved as RESs and diesel generators are non-renewable resources; their respective information has been reported in [12]. Noteworthy, battery charger capacities were not included in [12], while it is here fixed and is equal to half of its capacity. Moreover, EVs parking lot information was not reported in [12]; however, EVs parking lot capacity is 300 vehicles. Charger capacity, charge and discharge rates, and other EVs data exist in [6, 7]. Also, consumers participation rate in



**TABLE 2** Pareto front of the suggested strategy when  $\sigma = 0$ 

$\omega_{EEL}$	$\omega_{EENS}$	$\omega_{VSI}$	EEL (MWh)	EENS (MWh)	VSI (%)
1	0	0	1.755	3.893	20.75
0	1	0	1.894	1.472	20.14
0	0	1	1.849	4.038	22.43
0.5	0.5	0	1.825	2.507	20.44
0.5	0	0.5	1.809	3.719	21.82
0	0.5	0.5	1.855	2.794	21.19
0.33	0.33	0.33	1.845	2.926	21.26

the DRP is set at 30% [7]. Additionally, 16, 24, and 30 \$/MWh are energy prices in the DA energy market for consecutively intervals of 1–7 AM, 8 AM to 4 PM, 11–12 PM, and 5–10 PM [7].  $K_Q$  and  $K_R$  are fixed on 0.08, and 1, respectively. The load factor (power rate) is multiplied by the peak load (resource capacity) to provide load hourly information (generated power of RESs). The hourly data of EVs number is considered as the overall number of parking lot-linked EVs plus the EVs penetration rate. The daily curves of EVs penetration rate in the parking lot, power values of RESs, and load factor are presented in [4, 7].  $WSP^{min}$  is set at 0.8 [6]. The weak buses found by power flow are consecutive buses 67, 14, 12, and 14 in SDN, MG1, MG2, and MG3. Also, 60 scenarios are produced by the RWM for network component accessibility uncertainty. The network and MGs components values are set at 1%. It should be noted that the proposed scheme can be implemented on different networks and different sources and storage devices so that they can be implemented on real data.

## 4.2 | Simulation results

This section provides the results of the suggested strategy simulation in GAMS optimization software based on obtained information from Section 4.1, which is solved by the CPLEX [35]. The traditional piecewise linearization method involves 5 pieces. A regular 45-gon is likewise implemented for estimating the circular plane [21]. It can be seen from obtained results of [21] that the linear approximation model computational error of power and voltage in power flow optimization, prescribed as (1)–(10), are 2% and 0.5% compared to the non-linear power flow optimization. So it is ignored because of its small computational time [21].

### 4.2.1 | The best solution evaluation

Provided that the uncertainty level ( $\sigma$ ) is assumed zero for  $\omega_{EEL} = 0$ ,  $\omega_{EENS} = 0.33$ , and  $\omega_{VSI} = 0.5$ , the results of the Pareto front for the suggested strategy are given in Table 2. If all weighted coefficients are 1, the minimum values of EEL and EENS and maximum values of the VSI computed in this table are 1.755, 1.472, and 22.43 MWh, respectively. Remem-

**TABLE 3** The best solution of VSI, EENS, and EEL for different uncertainty levels

$\sigma$	EEL (MWh)	EENS (MWh)	VSI (%)	Calculation time (s)
0	1.803	1.936	22.10	13.5
0.1	1.922	2.067	22.06	14.4
0.2	2.088	2.253	22.02	15.2

ber that, VSI symmetry in (1) is shown by the term *min*; the aim of (1) is VSI maximization. The minimum EEL and EENS and maximum VSI are provided in these 3 cases. If the minimization of EENS in (1) is considered, the maximum EEL will be 1.894 MWh; if VSI symmetry minimization is regarded, the maximum EENS will be computed as 4.038 MWh; and if the minimization of EENS is assumed, the minimum VSI can be attained as 20.14 MWh. It can be assumed that 0.139 (1.894–1.755), 2.566 (4.038–1.472) MWh, and 2.29 (22.43–20.14) MWh are the change boundaries of the aforementioned functions. Besides, the change in these functions in Table 2 shows different trends. Indeed, as EEL increases, EENS proportionally decreases; minimizing EENS is associated with a great deal of supplied real power by sources, storages, and ALs; although line power loss may increase, subsequently, the expected energy loss increases.

By employing the weighted sum functions-based Pareto optimization method, the best solutions of VSI, EENS, and EEL for various uncertainty level values are listed in Table 3. If  $\sigma = 0$ , the VSI, EENS, and EEL values at the best solution will be 22.10, 1.936, and 1.803 MWh, respectively. The aforementioned values approximately equal their highest, least, and least values, where the distance between EEL and its least value is 34.5% ((1.803–1.755)/0.139), that of EENS is 18.1%, and that of VSI and its highest value is 14.4%. Finally, the weighted sum functions related to computational time are obtained by almost 13.5 s in Table 3.

It can be also seen from this table that increasing the uncertainty level ( $\sigma$ ) increases EEL and EENS values and decreases the VSI value compared to a case when  $\sigma = 0$ . According to Section 2.2, energy consumption by loads and EVs in the worst scenario ( $\sigma > 0$ ) can rise compared to a scenario with  $\sigma = 0$ , while the energy price and the real and reactive output power of the EVs will decrease. This leads to increased energy loss, voltage drops, and power outages in the network. Also, based on Section 2.2, it is expected that increasing the uncertainty level in the worst scenario will provide less response space than  $\sigma = 0$ . Therefore, the computational time of the suggested strategy increases in these conditions, as shown in Table 3.

### 4.2.2 | Evaluation of MGs financial condition

The expected revenue for MG1, MG2, and MG3 is depicted in Table 4 by considering flexibility tolerance changes ( $\Delta F$ ) and maximum EENS ( $EENS^{max}$ ). The tolerance curve of profit-flexibility of MGs for  $EENS^{max} = 1$  is considered in this table.

**TABLE 4** MGs expected revenue for different values of  $EENS^{max}$  and  $\Delta F$  ( $\sigma$  equals zero)

$\Delta F$ (MW) ( $EENS^{max} = 1$ MWh)		0	0.02	0.04	0.06	0.08	0.10
Expected profit (\$)	MG1	206	231	241	244	244	244
	MG2	629	663	676	681	681	681
	MG3	193	213	221	224	224	224
$EENS^{max}$ (MWh) for ( $\Delta F = 0$ )		1	3	5	7	9	11
Expected profit (\$)	MG1	206	239	258	266	268	268
	MG2	629	705	756	777	780	780
	MG3	193	222	241	249	250	250

**TABLE 5** MGs expected revenue for diverse cases and variant uncertainty levels

Parameter	$\Delta F$ (MW)			$EENS^{max}$ (MWh)			Profit (\$)			
	Uncertainty level	0	0.1	0.2	0	0.1	0.2	0	0.1	0.2
Case I	MG1	0	0	0	1	1	1	206	189	171
	MG2	0	0	0	1	1	1	629	575	520
	MG3	0	0	0	1	1	1	193	176	159
Case II	MG1	0.0218	0.0222	0.0225	3.09	3.46	3.93	262	241	219
	MG2	0.0216	0.0219	0.0222	3.07	3.42	3.90	741	682	631
	MG3	0.0219	0.0223	0.0227	3.09	3.47	3.94	244	225	208

As  $\Delta F$  increases based on the table, MGs expected revenue in the studied markets intensifies as the flexibility index significance is reduced here; consequently, the minimized operating cost of non-renewable resources, storage, and ALs is attained, leading to higher revenue for MGs (based on (13)). When  $\Delta F$  equals 0.06 MW, these trends are continued. The MGs expected revenue will be constant if  $\Delta F > 0.06$  MW. The curve of  $EENS^{max}$ -MGs revenue for  $\Delta F = 0$  is illustrated in this table as well. With the growth in  $EENS^{max}$ , since its increment broaden the problem solution space according to (26), the MGs expected revenue will increase as is shown in Table 4. The revenue becomes constant if  $EENS^{max} > 9$  MWh. Nevertheless, the suggested strategy cannot obtain the optimum solution when  $EENS^{max} < 1$  MWh; therefore, its respective results are excluded from Table 4.

The MGs financial condition is studied for two cases in Table 5:

- Employing the suggested strategy by MGs high flexibility and reliability condition ( $EENS^{max} = 1$  MWh,  $\Delta F = 0$ ) is considered as Case 1;
- Employing the suggested strategy as the best solution for MGs flexibility, reliability, and financial condition is considered as Case 2.

Firstly, MGs flexibility ( $\max(|P_{MGi,b,t,\omega} - P_{MGi,b,t,\omega'}|, \forall i, b, t, \omega, \omega')$ ), MGs EENS (left side of (26)), and MGs expected revenue, (13), are calculated for various values of  $EENS^{max}$  and  $\Delta F$ . Next, the fuzzy decision-making strategy is applied to

provide the best solutions. The MGs expected revenue in Case 2 is more than in Case 1 based on Table 5; however, MGs high reliability and flexibility are guaranteed in this case (lower  $EENS^{max}$  and  $\Delta F$ ). The  $EENS^{max}$  and  $\Delta F$  values respectively increase to 3.12 and 0.022 MWh in Case 2, while  $\sigma = 0$ . Since flexibility tolerance and  $EENS^{max}$  are small and MGs expected revenue is high, a situation for MGs flexibility, reliability, and financial indicators is determined. In addition, increasing the uncertainty level, compared to the case with  $\sigma = 0$ , reduces the MGs expected revenue in both case studies. In Case 2,  $EENS^{max}$  and  $\Delta F$  values are increased in a trade-off between the MGs financial, flexibility, and reliability status. This situation, according to Section 2.2, is due to the increment in energy consumption of the loads and EVs as well as energy price reduction, and a decrease in the real and reactive produced power of EVs in the worst scenario compared to  $\sigma = 0$ .

#### 4.2.3 | Evaluation of MGs operation

The MGs daily expected curve of the studied markets in Case 2 is depicted in Figure 2 for various  $\sigma$  values. Appropriately management of resources, storage, and ALs leads to real power injection of MGs to the SDN in every operational hour as well as financial profit from the energy market. Yet, less real power injection to the SDN can be observed based on this figure in the first operation hours (1–4 AM) and later energy programming hours (6–12 PM) in comparison with other times, because, according to the information in Section 4.1, the least amount

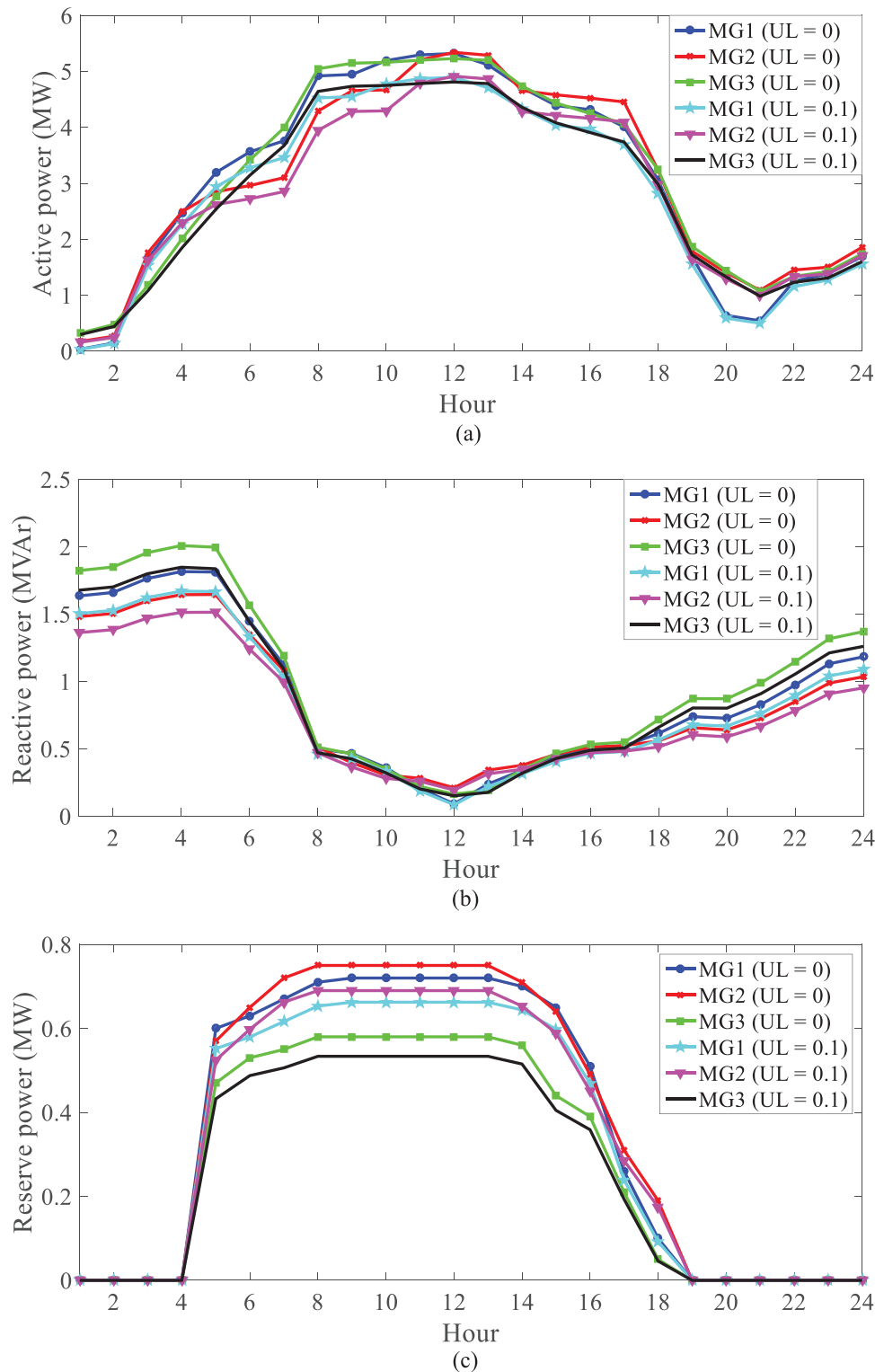


**FIGURE 2** a) Real, b) reactive, and c) reserve power-related daily expected curves of MGs for diverse uncertainty levels

of price of energy and the higher non-renewable resources fuel price (20\$/MWh) at 1–4 AM. As a result, batteries, EVs, and ALs will be users, and less power will be injected into MGs by non-renewable resources to minimize the costs of MGs. During 6–12 PM, there is a high network passive load, leading to

a heavily loaded network. Thus, less real power can be injected by MGs into the SDN. Note that a great portion of real power cannot be generated by the renewable resources between 1–4 AM and 6–12 PM, as is illustrated in [4], and PVs will be off in these durations. More real power can be injected into the SDN

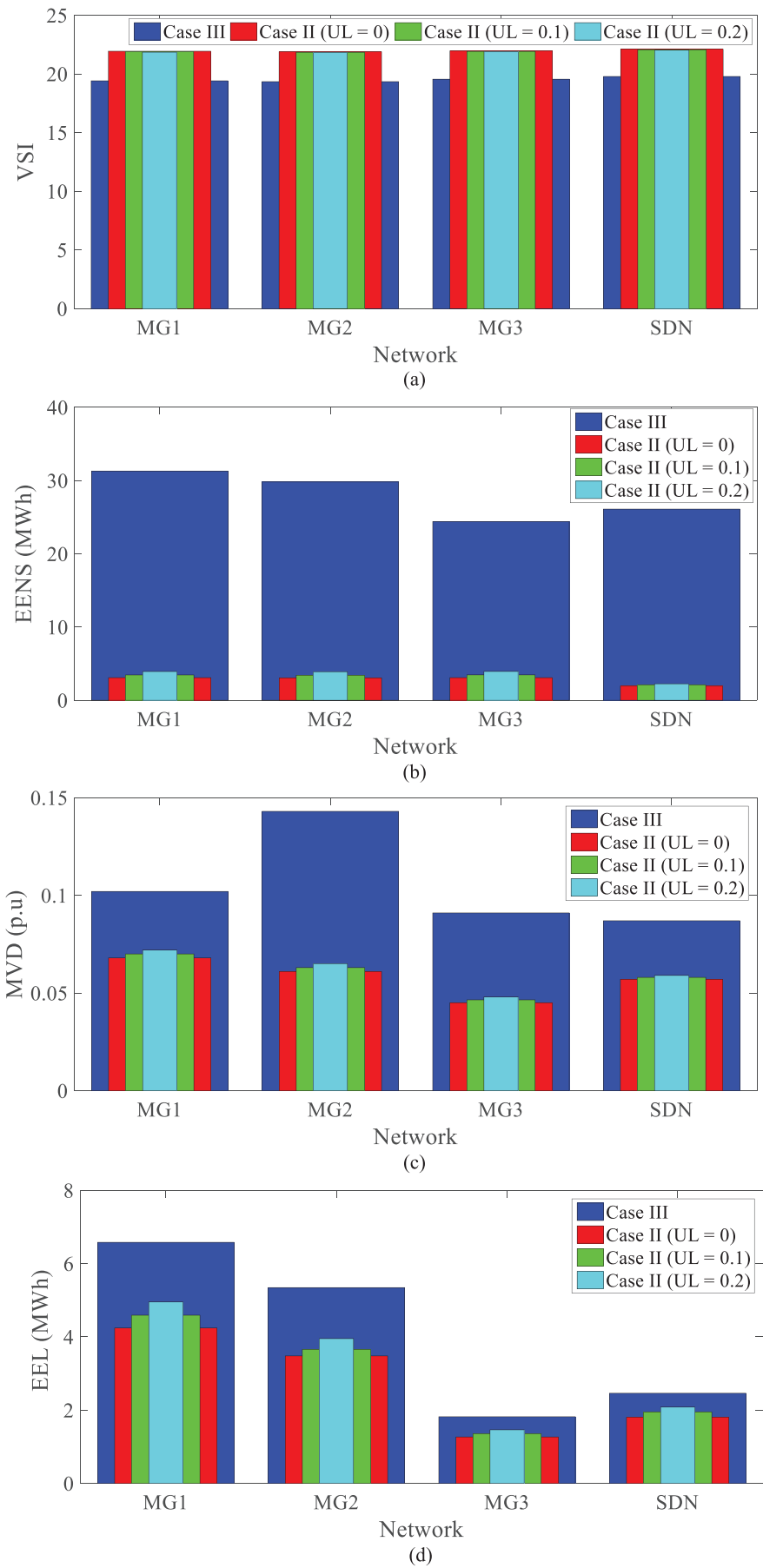


**FIGURE 3** a) VSI, b) EENS, c) MVD, d) EEL values in cases 3 and 4 for different uncertainty levels

by MGs from 5 AM to 5 PM because resources generate more power and the consumption of energy by loads, batteries, and EVs decreases.

Figure 2b shows the daily expected curve of reactive power of MGs in case 2 in which MGs generate reactive power, since, based on (16), they get powers of storage as well as non-renewable and renewable resources. MGs are considered generators of reactive power in the SDN because the number of reactive resources and their capacity in MGs is large based on Section 4.1. As shown in Figure 2a, more reactive power can be generated by MGs between 1–6 AM, when storage beside the ALs loads are charged. Consequently, more reactive power should be injected into MGs to avoid a significant decrease in voltage. Based on Figure 2a, a greater portion of resource capacity should be dedicated to real power generation during 7 AM to 12 PM. As the MGs reactive power is less in this interval, this leads to reduced reactive power generation by resources. Figure 2c exhibits the daily expected curve of MGs reserve power. Between 5–6 PM, if a greater portion of energy can be produced by resources in a way that a small portion of their capacity is allocated for reactive power generation, the reserve can be met by MGs. As mentioned, the MGs capacity is large enough to supply the reserve. The load consumption is high in the remaining intervals and a great portion of resources, storage, and ALs (only between peak hours) is considered for supplying the demand. For preventing an excessive decrease in voltage, a portion of the resource and storage capacities should be dedicated to generating reactive power. As a result, MGs capacity becomes smaller and cannot supply the reserve between 1–4 AM and 7–12 PM. Eventually, increasing the uncertainty level (UL or  $\sigma$ ) compared to  $\sigma = 0$ , leads to a downward shift of MGs daily curve of real, reactive, and reserve power as shown in Figure 3. The reason is that under these conditions, the load and EVs energy consumption increase, while the EVs capacity decreases to produce real and reactive power based on Section 2.2. Therefore, MGs can deliver less real, reactive, and reserve power to the SDN compared to a case with  $\sigma = 0$ .

#### 4.2.4 | Networks technical condition evaluation

The operation indices, that is, MGs and SDN reliability index (EENS), expected energy losses (EEL), maximum voltage drop (MVD), and voltage security index (VSI) are analysed in Figure 3 using 2 case studies (Case 3 and the power flow studies in Case 4) with diverse uncertainty levels (UL or  $\sigma$ ). The suggested strategy (Case 3) outperforms Case 4 in all network technical indices by using a better managing strategy for responsive loads, storage, and resources. In addition, VSI value equals 19.3–19.8 in Case 4, increases in other case, and is 21.8–22.0 for the worst scenario ( $\sigma = 0.2$ ). EENS in Case 4 is higher in the case of an  $N-1$  event (more than 24 MWh); however, EENS in Case 3 reduces to 3–4 MWh in the worst-case scenario. The suggested strategy is also able to reduce the MVD to 0.070 per unit at  $\sigma = 0.2$ . Finally, at  $\sigma = 0.2$ , the MG1, MG2, MG3 and SDN-associated energy loss mitigate to almost 32%

((6.6–4.5)/6.6), 35%, 30%, and 25% in Case 3 compared to Case 4, respectively. Moreover, the suggested strategy achieves more flexibility for MGs with the highest tolerance of 0.022 MW. Also,  $\Delta F$  would be 0 for 100% flexibility. In Case 3, the suggested strategy reaches high flexibility for MGs. Eventually, according to Figure 3, when uncertainty levels are smaller than 0.2, the improvement conditions of the mentioned indicators in Case 3 are more favourable than in  $\sigma = 0.2$  according to Section 2.2. At a higher uncertainty level, the energy consumed in the grid is higher, and their resources produce less energy, leading to higher amount of energy received from the upstream network. This results in higher energy loss, voltage drop, EENS, and lower VSI than the case with  $\sigma = 0$ .

## 5 | CONCLUSION

A two-level power management strategy was proposed for SDN and MGs that considers MGs participation in the day-ahead energy, reactive power, and reserve market. The first layer considered SDN optimum programming according to the power management strategy of lower level (that coordinates DSO with MG operators) by multi-objective functions including minimization of security index symmetry, EENS, and energy loss. Weighted sum functions-based Pareto optimization was implemented to formulate a problem subject to linearized AC-power flow relationships and voltage security and reliability constraints. Besides, the model of MGs participation in the aforementioned markets according to the power management strategy of the lower level (that coordinates MG operators with loads, storage, and resources) was illustrated; its objective function goal was the minimization of the difference between expected cost of non-renewable resources and the expected profit of MGs constrained by the model, flexibility, operation, reliability, and security of the MG. To establish a single-level problem, the KKT strategy was utilized, and hybrid stochastic-robust programming was employed for modelling the uncertainties of mobile storage energy demand, renewable power, load, network component accessibility, and price of energy. Finally, evaluation of numerical results showed that the weighted sum functions strategy is able to search the solution, that is, the almost minimum values of VSI symmetry, EENS, and loss of energy. In addition, the highest flexibility tolerance of 0.022 MW was obtained in comparison with the worst scenario, that is, the maximum uncertainty level (0.2). By comparing the power flow studies, high values of EENS, VSI, MVD, and energy loss can be mitigated by the suggested strategy to 3–4 MWh, to 22, to below 0.070 per-unit, and to 30%, respectively.

## NOMENCLATURE

### Abbreviation

DA	Day-ahead
DRP	Demand response program
DSO	Distribution system operator
EEL	Expected energy loss

EENS	Expected energy not-supplied
EMS	Energy management system
EV	Electric vehicle
KKT	Karush–Kuhn–Tucker
MG	Microgrid
MGO	Microgrid operator
MMG	Multi-microgrid
MOV	Maximum overvoltage
MVD	Maximum voltage drop
PMS	Power management system
RES	Renewable energy source
RWM	Roulette wheel mechanism
SBM	Simultaneous backward method
SDN	Smart distribution network
VSI	Voltage security index
WSI	Worst security index

### Indicators and sets

$b, i, t, \omega$	Bus, MG, operation hour, and scenario indicators
$j$	Bus auxiliary index
$p, m$	The piecewise linear index of the traditional piecewise linearization strategy; a side index of a regular polygon
$pb, pb-1$	The weak bus and its upstream bus
$O_B, O_{MG}, O_{OH}, O_S$	Buses, MGs, operation hours, and scenario sets
$O_B^{MG}$	MG buses set
$O_p, O_M$	The piecewise linear set of the traditional piecewise linearization strategy; a regular polygon side set

### Variables

$EEL, EENS, VSI$	Expected energy loss (MWh), expected energy not-supplied (MWh), and voltage security index (dimensionless)
$F_1$	The energy loss sum, expected energy not-supplied, and voltage security according to the weighted sum functions strategy (dimensionless)
$F_2$	The difference between the expected non-renewable resources operational cost and MGs expected profit from understudied markets (\$)
$L_{NS}$	Real power not-supplied (p.u.)
$P_{CH}, P_{DIS}$	Real power of storage system charging and discharging (p.u.)
$P_{DS}, P_{MG}, P_L$	Real power of the SDN's and MG's substation, and distribution line
$P_{NR}, P_{DR}$	Real power of non-renewable resources and active power of responsive loads in the demand response program (p.u.)

$Q_{DS}, Q_{MG}, Q_L, Q_{NR}, Q_R, Q_E$	Reactive power of the SDN's and MG's substation, distribution line, non-renewable and renewable resources, and storage charger (p.u.)
$R_{MG}$	Reserve power of the MG observed by the MG's substation (p.u.)
$V, \Delta V$	voltage magnitude and deviation (p.u.)
$WSI$	The worst security index (dimensionless)
$\varphi$	Voltage angle (rad)

### Constants

$A_L$	The incidence matrix of buses and distribution lines (if there is a line between buses $b$ and $j$ , $A_{L,bj} = 1$ , otherwise, it is equal to zero)
$A_{MG}$	The incidence matrix of MGs and buses in the SDN (if MG $i$ connects to bus $b$ , $A_{MG,b,i} = 1$ , otherwise it is equal to zero)
$B_L, G_L$	Susceptance and conductance of the distribution line (p.u.)
$\underline{E}, \bar{E}, IE$	Minimum storable energy, capacity (maximum storable energy), and initial energy of the storage (MWh)
$EENS^{max}$	Maximum energy not-supplied (MWh)
$K_Q, K_R$	The ratio between the reactive power price and the energy price, the ratio between the reserve price and the energy price (dimensionless)
$L_p, L_Q$	Real and reactive power of load (p.u.)
$n_p$	The number of linear pieces in the traditional piecewise linearization strategy
$P_R$	Real power of the renewable resource (p.u.)
$R, X$	Resistance and reactance of the distribution line (p.u.)
$s, s'$	The slope of the line used for linearizing a second and fourth power variable based on the conventional piecewise linearization technique
$\bar{S}_{DS}, \bar{S}_{MG}, \bar{S}_L, \bar{S}_{NR}, \bar{S}_R, \bar{S}_E$	Size (maximum apparent power) of the SDN's substation, MG's substation, distribution line, non-renewable and renewable resources, and storage charger (p.u.)
$V_{min}, V_{max}$	Lower and upper limits of voltage magnitude (p.u.)
$WSI^{min}$	The minimum value of WSI

$\alpha_{CR}, \alpha_{DR}$	Charging and discharging rates of the storage (p.u.)
$\beta$	Fuel price of the non-renewable resource (\$/MWh)
$\beta_{DS}, \beta_{MG}, \beta_L$	Accessibility of the SDN's and MG's substation, and distribution line
$\gamma$	Energy price (\$/MWh)
$\eta_{CH}, \eta_{DIS}$	Charging and discharging efficiency of the storage device
$\pi$	The probability of occurrence of a scenario
$\vartheta_{EEL}, \vartheta_{EENS}, \vartheta_{VSI}$	Weighted coefficients
$\xi$	The participation rate of consumers in the DRP
$\Delta F$	Flexibility tolerance
$\Delta\theta, n_m$	Angle deviation (rad), and the number of sides of the regular polygon, $\Delta\theta = 360/n_m$

## AUTHOR CONTRIBUTIONS

Mehdi Veisi: Conceptualization, Investigation, Software, Validation. Farid Adabi: Project administration, Supervision. Abdollah Kavousi-Fard: Formal analysis, Supervision, Writing original draft. Mazaher Karimi: Resources, Writing review & editing.

## ACKNOWLEDGEMENTS

The REDISET project has supported the work of Mazaher Karimi with the financial support provided by Business Finland with Grant No. 27081089141/REDISET/WP/2704800. The financial support provided through the research project is highly acknowledged.

## CONFLICT OF INTEREST

The authors declare that there is no conflict of interest that could be perceived as prejudicing the impartiality of the research reported.


## DATA AVAILABILITY STATEMENT

Data sharing not applicable. No new data were created or analysed in this study.

## ORCID

Mehdi Veisi  <https://orcid.org/0000-0001-7375-8267>

Farid Adabi  <https://orcid.org/0000-0002-5159-8909>

Abdollah Kavousi-Fard  <https://orcid.org/0000-0001-8316-5588>

Mazaher Karimi  <https://orcid.org/0000-0003-2145-4936>

## REFERENCES

- Kiani, H., Hesami, K., Azarhooshang, A.R., Pirouzi, S., Safaei, S.: Adaptive robust operation of the active distribution network including renewable and flexible sources. *Sustainable Energy Grids Networks* 26, 100476 (2021)
- Kavousi-Fard, A., Khodaei, A.: Efficient integration of plug-in electric vehicles via reconfigurable microgrids. *Energy* 111, 653–663 (2016)
- Bollen, M.: The smart grid: Adapting the power system to new challenges. In: *The Smart Grid: Adapting the Power System to New Challenges*. Morgan & Claypool, San Rafael, CA (2011)
- Norouzi, M.A., Aghaei, J., Pirouzi, S., Niknam, T., Lehtonen, M.: Flexible operation of grid-connected microgrid using ES. *IET Gener. Transm. Distrib.* 14(2), 254–264 (2019)
- Hu, X., Liu, T.: Co-optimisation for distribution networks with multi-microgrids based on a two-stage optimisation model with dynamic electricity pricing. *IET Gener. Transm. Distrib.* 11(9), 2251–2259 (2017)
- Pirouzi, S., Aghaei, J.: Mathematical modeling of electric vehicles contributions in voltage security of smart distribution networks. *Simulation* 95(5), 429–439 (2019).
- Norouzi, M.A., et al.: Hybrid stochastic/robust flexible and reliable scheduling of secure networked microgrids with electric springs and electric vehicles. *Appl. Energy* 300, 117395 (2021)
- Rasouli, A., Bigdeli, M., Samimi, A.: Robust particle swarm optimization for active/reactive and reserve scheduling in a grid-connected microgrid with energy storage systems. *Int. J. Energy Res.* 45, 19331–19350 (2021)
- Azarhooshang, A.R., Sedighzadeh, D., Sedighzadeh, M.: Two-stage stochastic operation considering day-ahead and real-time scheduling of microgrids with high renewable energy sources and electric vehicles based on multi-layer energy management system. *Electr. Power Syst. Res.* 201, 107527 (2021)
- Homayoun, R., et al.: Multi-objective operation of distributed generations and thermal blocks in microgrids based on energy management system. *IET Gener. Transm. Distrib.* 15(9), 1451–1462 (2020)
- Roustaei, M., Kazemi, A.: Multi-objective energy management strategy of unbalanced multi-microgrids considering technical and economic situations. *Sustainable Energy Technol. Assess.* 47, 101448 (2021)
- Hamzeh-Aghdam, F., Ghaemi, S., Taghizadegan-Kalantari, N.: Evaluation of loss minimization on the energy management of multi-microgrid based smart distribution network in the presence of emission constraints and clean productions. *J. Cleaner Prod.* 196, 185–201 (2018)
- Samimi, A., Shateri, H.: Network constrained optimal performance of DER and CHP based micro-grids within an integrated active-reactive and heat powers scheduling. *Ain Shams Eng. J.* 12, 3819–3834 (2021)
- Zhang, C., Xu, Y., Dong, Z.Y.: Robustly coordinated operation of a multi-energy micro-grid in grid-connected and islanded modes under uncertainties. *IEEE Trans. Sustainable Energy* 11(2), 640–651 (2020)
- Accetta, A., Pucci, M.: Energy management system in DC micro-grids of smart ships: Main gen-set fuel consumption minimization and fault compensation. *IEEE Trans. Ind. Appl.* 55(3), 3097–3113 (2019)
- Parhizi, S., Khodaei, A., Shahidehpour, M.: Market-based versus price-based microgrid optimal scheduling. *IEEE Trans. Smart Grid* 9(2), 615–623 (2018)
- Pirouzi, S., et al.: Power conditioning of distribution networks via single-phase electric vehicles equipped. *IEEE Syst. J.* 13(3), 3433–3442 (2019)
- Roustaei, M., Kazemi, A.: Multi-objective stochastic operation of multi-microgrids constrained to system reliability and clean energy based on energy management system. *Electr. Power Syst. Res.* 194, 106970 (2021)
- Abrisham-Foroushan-Asl, S., Bagherzadeh, L., Pirouzi, S., Norouzi, M.A., Lehtonen, M.: A new two-layer model for energy management in the smart distribution network containing flexi-renewable virtual power plant. *Electr. Power Syst. Res.* 194, 107085 (2021)
- Shahbazi, A., et al.: Holistic approach to resilient electrical energy distribution network planning. *Int. J. Electr. Power Energy Syst.* 132, 107212 (2021)
- Bozorgavari, S.A., Aghaei, J., Pirouzi, S., Nikoobakht, A., Farahmand, H., Korpås, M.: Robust planning of distributed battery energy storage systems in flexible smart distribution networks: A comprehensive study. *Renewable Sustainable Energy Rev.* 123, 109739 (2020)
- Afrashi, K., Bahmani-Firouzi, B., Nafar, M.: IGDT-based robust optimization for multicarrier energy system management. *Iran. J. Sci. Technol., Trans. Electr. Eng.* 45(1), 155–169 (2021)
- Aghaei, J., Amjadi, N., Baharvandi, A., Akbari, M.A.: Generation and transmission expansion planning: MILP-based probabilistic model. *IEEE Trans. Power Syst.* 29(4), 1592–1601 (2014)

24. Kavousi-Fard, A., Khodaei, A.: Multi-objective optimal operation of smart reconfigurable distribution grids. *AIMS Energy* 4(2), 206–221 (2016)
25. Chen, X., Su, W., Kavousi-Fard, A., Skowronska, A.G., Mourelatos, Z.P., Hu, Z.: Resilient microgrid system design for disaster impact mitigation. *Sustainable Resilient Infrastruct.* 6, 56–72 (2021)
26. Kavousi-Fard, A., Abbasi, S., Abbasi, A.R., Tabatabaie, S.: Optimal probabilistic reconfiguration of smart distribution grids considering penetration of plug-in hybrid electric vehicles. *J. Intell. Fuzzy Syst.* 29(5), 1847–1855 (2015)
27. Kavousi-Fard, A., Niknam, T.: Optimal distribution feeder reconfiguration for reliability improvement considering uncertainty. *IEEE Trans. Power Delivery* 29(3), 1344–1353 (2014)
28. Malekpour, A.R., Niknam, T., Pahwa, A., Kavousi Fard, A.: Multi-objective stochastic distribution feeder reconfiguration in systems with wind power generators and fuel cells using the point estimate method. *IEEE Trans. Power Syst.* 28(2), 1483–1492 (2013)
29. Hamidpour, H.R., et al.: Integrated resource expansion planning of wind integrated power systems considering demand response programmes. *IET Renewable Power Gener.* 13(4), 519–529 (2018)
30. Babu, P.R., Rakesh, C.P., Srikanth, G., Kumar, M.N., Reddy, D.P.: A novel approach for solving distribution networks. In: *India Conference (INDICON), 2009 Annual IEEE*. Gandhinagar, India, pp. 1–5 (2009)
31. Aghaei, J., et al.: Flexibility planning of distributed battery energy storage systems in smart distribution networks. *Iran. J. Sci. Technol., Trans. Electr. Eng.* 44(3), 1105–1121 (2020)
32. Pirouzi, S., Latify, M.A., Yousefi, G.R.: Investigation on reactive power support capability of PEVs in distribution network operation. In: *23rd Iranian Conference on Electrical Engineering*. Tehran, Iran, pp. 1591–1596 (2015)
33. Ansari, M.R., et al.: Renewable generation and transmission expansion planning coordination with energy storage system: A flexibility point of view. *Appl. Sci.* 11(8), 3303 (2021)
34. Dini, A., et al.: Security-constrained generation and transmission expansion planning based on optimal bidding in the energy and reserve markets. *Electr. Power Syst. Res.* 193, 107017 (2021)
35. Generalized algebraic modeling systems (GAMS). [online], 2015, available: <http://www.gams.com/2015>

**How to cite this article:** Veisi, M., Adabi, F., Kavousi-Fard, A., Karimi, M.: A novel comprehensive energy management model for multi-microgrids considering ancillary services. *IET Gener. Transm. Distrib.* 1–16 (2022).  
<https://doi.org/10.1049/gtd2.12632>